ISSN: 2228-7922
Journal of Computational and Applied Research in Mechanical Engineering
Vol. 10, No. 1, pp. 171-181
jcarme.sru.ac.ir

# Impact of thermal radiation and viscous dissipation on hydromagnetic unsteady flow over an exponentially inclined preamble stretching sheet

**S. R. R. Reddy and P. B. A. Reddy***

*Department of Mathematics, S.A.S., Vellore Institute of Technology, Vellore-632014, India.*

**Article info:**
Type: Research
Received: 08/06/2018
Revised: 25/09/2019
Accepted: 01/10/2019
Online: 05/10/2019

**Keywords:**
Stretching sheet,
Permeability parameter,
Thermal radiation,
Non-uniform heat source or sink,
Chemical reaction.

**Abstract**
The present numerical attempt deals with the sway to transfer of heat and mass characteristics on the time-dependent hydromagnetic boundary layer flow of a viscous fluid over an exponentially inclined preamble stretching sheet. Furthermore, the role of viscous heating, thermal radiation, uneven energy gain or loss, velocity slip, thermal slip and solutal slips are depicted. The prevailing time-dependent PDE's are rehabilitated into coupled non-linear ODE's with the aid of apposite similarity transformations and then revealed numerically by using the 4th order R-K method incorporated with shooting scheme. Influence of various notable parameters like porosity, inertia coefficient, radiation, Eckert number, velocity, thermal and solutal slip are explored via graphs and tables for the cases assisting and opposing flows. Comparison amid the previously published work and the present numerical outcomes for the limiting cases are in a righteous agreement. Temperature increments with large values of the non-uniform heat source.

## 1. Introduction

The boundary layer flow over an extending sheet problem has been actively premeditated for decades because of its extensive applications in technology and industry. Few of these applications are, for example, streamlined expulsion of plastic sheets, hot rolling, MHD generators, accelerators, paper manufacture, artificial fibers, drawing of copper wires, glass blowing, metal turning, drawing plastic films, electronic cooling devices and numerous others. The examination of flow over an extending sheet was pioneered by Crane [1]. Many researchers [2-19] have scrutinized various behaviors of flow in stretching surfaces. These studies were affected by the stretching surfaces where thought to be unfaltering. Few attempts [19–23] have been carried out to describe the unsteady flows in connection with the stretching surfaces. Bachok et al. [24] mentioned the unsteady laminar physical phenomenon flow over a ceaselessly stretching porous surface. The transfer of heat behavior in the unsteady, laminar, incompressible viscous fluid over an extending permeable surface was analyzed by Pal [25]. Misra and Sinha [26] reported the impact of the hydromagnetic flow of blood in porosity in an extensive motion. Srinivas et al. [27] explored the Non-Darcian fluid flow over a permeable extending sheet.
MHD issues occur in a few circumstances like the prediction of room climate, Stream rate estimation and refreshment in nourishment

*Corresponding author
email address: pbarmaths@gmail.com

industry. Likewise, MHD is used in geophysics techniques, stellar structures, solar panel, designing MHD pumps, radio communication, interstellar issue, etc. Yan Zhang et al. [28] analyzed the thin liquid film flow over an unsteady extending surface in the presence of a variable magnetic field. Hatami et al. [29] studied the unsteady hydromagnetic Couette flows between two parallel infinite plates by utilizing the Differential Transformation Method (analytical method) and Differential Quadrature Method (numerical method). Plasma can be made to collaborate with the magnetic and adjust transfer of heat and erosion trademark. Since few liquids can also emit and absorb thermal radiation, in such circumstance, investigating the influence of magnetic field on the temperature distribution and transfer of heat when the liquid is not just an electrical conduit yet, in addition, it is equipped for transmitting and engrossing thermal radiation has turned into more prominent significance in space applications. Uneven energy gain or loss exhibits a behavior to change the heat dissipation in fluid which consequently affect the molecule statement rate in the framework; for example, semiconductor devices, electronic devices, and atomic pile. Heat source/sink might be viewed as steady, spaceward or heat subordinate. Here, we will examine the space and temperature dependent heat source/sink. Ghadikolaei et al. [30] investigated unsteady 2D squeezing flow of hydromagnetic fluid between two parallel infinite plates with heat generation/absorption.

The present model exhibits the impact of chemically reacting hydromagnetic flow over an inclined exponentially stretching surface using uneven gain/loss. To the author's consciousness, no exploration has been done until now in the literature about the influence of slips, viscous dissipation and chemical reaction in an inclined exponentially stretching surface. Such investigations are of awesome significance to engineers and scientists on account of their relatively all-inclusive event in numerous parts of science and engineering. A couple of representative fields of attention in which the transfer of heat and transfer of mass along with chemical reaction in the boundary layer flow has many practical applications includes the conveyance of heat and wetness over agribusiness fields and forests of organic product trees, damage of crops because of solidifying, flow in a desert cooler and so on. Enthused by the above studies and the potential applications, a mathematical model is presented here to comprehend the heat and mass characteristics of unsteady hydromagnetic flow of a viscous fluid over an inclined exponentially porous extending surface.

## 2. Mathematical formulation

Let us consider the two-dimensional(x,y) time dependent hydromagnetic boundary layer flow of a viscous fluid over an exponentially inclined preamble stretching sheet with an acute angle $\delta$ to the vertical. Fig. 1 Shows the coordinate system and flow model. At the time $t=0$, the sheet is impulsively stretched with velocity $U_w(x,t)$. A magnetic field *B(t)* is implemented normal to the sheet. The first-order homogeneous time-dependent chemical reaction, solutal, thermal and velocity slip have been taken into account. Then in the view of these boundary layer conventions, the continuity, momentum, energy and concentration species can be conveyed as (Magyari and Keller [5], Pal [7], Reddy and Reddy [21] and Chamkha et al. [22]):

$$\frac{\partial u}{\partial x}+\frac{\partial v}{\partial y}=0, \tag{1}$$

$$\frac{\partial u}{\partial t}+u\frac{\partial u}{\partial x}+v\frac{\partial u}{\partial y}=\upsilon\frac{\partial^2 u}{\partial y^2} +\left(\beta\left(T-T_\infty\right)+\beta^*\left(C-C_\infty\right)\right)g\cos\delta -\frac{\sigma B^2}{\rho}u-\frac{v}{k_1}u-F^*u^2, \tag{2}$$

$$\frac{\partial T}{\partial t}+u\frac{\partial T}{\partial x}+v\frac{\partial T}{\partial y}=\frac{k}{\rho c_p}\frac{\partial^2 T}{\partial y^2} +\frac{\mu}{\rho c_p}\left(\frac{\partial u}{\partial y}\right)^2-\frac{1}{\rho c_p}\frac{\partial q_r}{\partial y}+\frac{q'''}{\rho c_p}, \tag{3}$$

$$\frac{\partial C}{\partial t}+u\frac{\partial C}{\partial x}+v\frac{\partial C}{\partial y}=D\frac{\partial^2 C}{\partial y^2}-\Gamma\left(C-C_\infty\right). \tag{4}$$

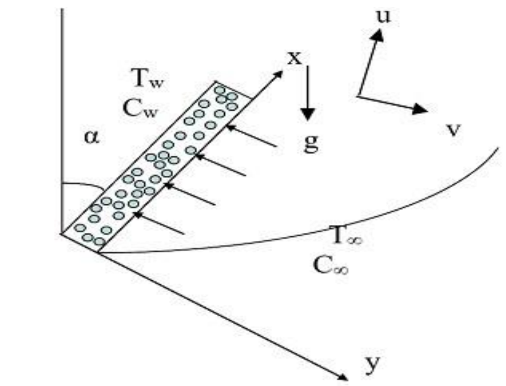


**Fig. 1.** Physical model of the problem.

The boundary conditions of aforementioned governing equations are

$$u = U_w + N\mu\frac{\partial u}{\partial y}, v = -V_w,$$
$$T = T_w + M_1\frac{\partial T}{\partial y}, C = C_w + P\frac{\partial C}{\partial y} \quad \text{at } y = 0, \tag{5}$$
$$u \to 0, T \to T_\infty, C \to C_\infty \quad \text{as } y \to \infty.$$

where $V_w, k_1, N, M_1, \Gamma, B, P, U_w, T_w$ and $C_w$ are

$$V_w = f_0\sqrt{\frac{U_0\upsilon}{2L(1-\alpha t)}}e^{\frac{x}{2L}}, k_1 = k_2(1-\alpha t)e^{\frac{-x}{L}},$$
$$N = N_0(1-\alpha t)^{\frac{1}{2}}e^{\frac{-x}{2L}}, M_1 = M_0(1-\alpha t)^{\frac{1}{2}}e^{\frac{-x}{2L}},$$
$$\Gamma(t) = \Gamma_0(1-\alpha t)^{-1}e^{\left(\frac{x}{L}\right)}, B = B_0(1-\alpha t)^{-\frac{1}{2}}e^{\left(\frac{x}{2L}\right)},$$
$$P = P_0(1-ct)^{\frac{1}{2}}e^{\frac{-x}{2L}}, U_w = \frac{U_0}{(1-\alpha t)}e^{\frac{x}{L}},$$
$$T_w = T_\infty + \frac{T_0}{1-\alpha t}e^{\frac{x}{2L}}, C_w = C_\infty + \frac{C_0}{1-\alpha t}e^{\frac{x}{2L}}. \tag{6}$$

The non-uniform heat source/sink, $q'''$ is modelled as:

$$q''' = \frac{kU_w}{2L\upsilon}\left[A^*(T_w - T_\infty)f' + B^*(T - T_\infty)\right]. \tag{7}$$

The radiative heat flux $q_r$ is given by:

$$q_r = -\frac{4\sigma^*}{3k^*}\frac{\partial T^4}{\partial y}. \tag{8}$$

where $k^*$ and $\sigma^*$ are the Stefan–Boltzmann constant and Rosseland mean absorption coefficient respectivelly. The changes of heat discrepancies in the mass of blood flow are trivial. By ignoring higher order terms, Eq. (8) can be linearized by expanding $T^4$ into Taylor's series about $T_\infty$ then we get:

$$T^4 \cong 4T_\infty^3 T - 3T_\infty^4. \tag{9}$$

Invoking Eqs. (7, 8 and 9), Eq. (3) can be written as:

$$\frac{\partial T}{\partial t} + u\frac{\partial T}{\partial x} + v\frac{\partial T}{\partial y} = \left(\frac{k}{\rho c_p} + \frac{16\sigma^* T_\infty^3}{3\rho C_p k^*}\right)\frac{\partial^2 T}{\partial y^2}$$
$$+\frac{kU_w(x,t)}{2L\rho c_p\upsilon}\left[A^*(T_w - T_\infty)f' + B^*(T - T_\infty)\right] \tag{10}$$
$$+\frac{\mu}{\rho c_p}\left(\frac{\partial u}{\partial y}\right)^2$$

The following similarity transformation is introduced:

$$\eta = \left(\frac{U_0}{2\upsilon L(1-\alpha t)}\right)^{\frac{1}{2}}e^{\frac{x}{2L}}y, \psi = \left(\frac{2U_0\upsilon L}{(1-\alpha t)}\right)^{\frac{1}{2}}e^{\frac{x}{2L}}f(\eta),$$
$$T = T_\infty + \frac{T_0}{1-\alpha t}e^{\frac{x}{2L}}\theta(\eta), \ C = C_\infty + \frac{C_0}{1-\alpha t}e^{\frac{x}{2L}}\varphi(\eta). \tag{11}$$

Now, introduce $\psi$ function which is expressed as:

$$\text{as } u = \frac{\partial\psi}{\partial y}, \ v = -\frac{\partial\psi}{\partial x}, \tag{12}$$

Now, substituting Eqs. (11 and 12) into the Eqs. (2, 4, and 10) leads to:

$$f''' - 2(f')^2 + ff'' - (\eta f'' + 2f')A$$
$$+(Gr\ \theta + Gc\ \phi)\cos\delta - (M + K)f' \tag{13}$$
$$-F(f')^2 = 0,$$

$$\left(1 + \frac{4}{3}R\right)\theta'' - \Pr(f'\theta - f\theta') - \Pr A(\eta\theta' + 2\theta)$$
$$+Ec\Pr(f'')^2 + B^*\theta + A^* f' = 0, \tag{14}$$

$$\frac{1}{Sc}\phi''+f\phi'-f'\phi-A\left(2\phi+\eta\phi'\right)-\gamma\phi=0\,. \quad (15)$$

with dimensionless boundary conditions of

$$\left.\begin{array}{l} f=f_0,\; f'=1+S_f f''(0), \\ \theta=1+S_t\theta'(0), \phi=1+S_c\phi'(0) \end{array}\right\} \text{at}\, \eta=0, \qquad (16)$$
$$f'\to 0, \theta\to 0, \phi\to 0 \qquad as\,\eta\to\infty.$$

where the non-dimensional parameters are given by

$$Gr=\frac{2g\beta L(T_w-T_\infty)}{U_w^2}, Gc=\frac{2g\beta^* L(C_w-C_\infty)}{U_w^2},$$
$$A=\frac{\alpha L}{U_w(1-\alpha t)},\; M=\frac{2L\sigma B_0^2}{\rho U_0}, F=2F^*L,$$
$$K=\frac{2\upsilon L}{k_2 U_0},\; R=\frac{4\sigma^* T_\infty^3}{kk^*}, Ec=\frac{U_w^2}{(T_w-T_\infty)c_p}, \qquad (17)$$
$$\Pr=\frac{\mu c_p}{k}, Sc=\frac{\nu}{D} \text{ and } \gamma=\frac{2L\Gamma_0}{U_0}.$$

$Gc$ solutal Grashof number, $Gr$ is the Grashof number, $A$ is the unsteadiness parameter, $M$ is the magnetic parameter, $F$ is the dimensionless inertia coefficient, $K$ is the permeability parameter, $R$ is the radiation parameter, $Ec$ Eckert number, $Pr$ is the Prandtl number, $\gamma$ is the chemical reaction parameter. The parameters $Gc$, $Gr$ $A$ and $Ec$ are treated as local dimensionless parameters.

In Eq. (16), $f_0<0$ correspond to injection and $f_0>0$ correspond to suction. The solutal slip $S_c$ thermal slip $S_t$ and velocity slip $S_f$, are as

$$S_f=N_0\rho\sqrt{\frac{\upsilon U_0}{2L}}, S_t=M_0\sqrt{\frac{U_0}{2\upsilon L}} \text{ and}$$
$$S_c=P_0\sqrt{\frac{U_0}{2\upsilon L}}\;. \qquad (18)$$

In the equations written above, primes denote derivatives with respect to $\eta$.

The dimensionless skin friction factor $\left(C_f\right)$, rate of heat transfer $\left(Nu_x\right)$ and rate of mass transfer $\left(Sh_x\right)$ are defined as:

$$C_f=\frac{2\mu\left(\frac{\partial u}{\partial y}\right)_{y=0}}{\rho U_w^2}=\sqrt{2}\,\text{Re}_x^{-\frac{1}{2}} f''(0), \qquad (19)$$

$$Nu_x=-\frac{x\left(1+\frac{16\sigma^* T_\infty^3}{3kk^*}\right)\left(\frac{\partial T}{\partial y}\right)_{y=0}}{(T_w-T_\infty)} \qquad (20)$$
$$=-\text{Re}_x^{\frac{1}{2}}\left(1+\frac{4}{3}R\right)\theta'(0),$$

$$Sh_x=\frac{x\left(\frac{\partial C}{\partial y}\right)_{y=0}}{(C_w-C_\infty)}=-\text{Re}_x^{\frac{1}{2}}\varphi'(0). \qquad (21)$$

where $\text{Re}_x=\frac{LU_w}{\upsilon}$ is the local Reynolds number.

## 3. Results and discussion

The non-remittal values of the various parameters were measured as $M$ = 1.0, $Gr$ = 2.0, $Gc$ = 2.0, $A$ = 1.0, $\delta=\frac{\pi}{4}$, $F$ = 0.5, $K$ = 2.0, $A^*$ =-0.5, $R$ = 0.5, $B^*$ = -0.5, $Pr$ = 0.72, $Ec$ = 0.5, $Sc$ = 0.60, $f_0$ = 0.5, $\gamma=0.5$, $S_f=0.5$, $S_t=0.5$ and $S_c=0.5$, unless otherwise stated. The Velocity( $f'$ ), temperature ( $\theta$ ) and concentration ( $\phi$ ) for numerous values of parameters $M, A, K, Gr, Gc, \delta, F, S_f, R, A^*, B^*, Ec, S_c, Pr, Sc, \gamma, f_0$ and $S_t$ are portrayed in Figs. 2-6. Fig. 2(a) elucidates that the velocity diminishes with the higher values of M for the cases of opposing, assisting and time-dependent. It is noted that the larger value of M significantly enhances due to Lorentz force. The differences in the $f'$ for variations in the $Gc$ are displayed in Fig. 2(b). From this figure, it very well may be construed that an expansion in the $Gc$ upgrades the speed for opposing, assisting and steady-state cases. Fig. 2(c) depicts the disparity of velocity distribution for various estimations of $S_f$. It is perceived that the velocity of the boundary layer declines with elevating $S_f$ [21]. The impact of the permeability parameter on the $f'$ is displayed in Fig. 2(d). It tends to be seen that an expansion in the permeability parameter improves the speed. Fig. 2(e) presents the difference of $f'$ with various values of dimensionless inertia coefficient. Results expose that the $f'$ diminishes with a rise in the dimensionless inertia coefficient. The dimensionless velocity transferences for various estimations of the inclination parameter are shown in Fig. 2(f). Results show that the velocity diminishes with the expanding inclination parameter for unsteady and steady-state cases.

Fig. 3(a-f) shows the temperature distribution for different estimations of thermal radiation, Eckert number, thermal slip, Prandtl number and heat generation/absorption. The characteristic of $R$ on temperature profile is portrayed in Fig. 3(a) for three different cases. From this, it very well may be deduced that the fluid temperature is enhanced by rising the radiation parameter. Fig. 3(b) is planned to reveal insights into the impact of Eckert number on the fluid temperature. It is found that the higher values of Eckert number lead to enhance the fluid temperature. It is revealed that the thermal energy is saved in the fluid by frictional heating. It is due to the reason that the larger value of the Eckert numbers is raising the temperature at each point in the fluid. Fig. 3(c) portrays thermal slip impacts on temperature profile for three cases. In this, it tends to be seen that the temperature-related boundary layer thickness lessens with expanding values of velocity slip parameter. Fig. 3(d) characterizes the progressions of temperature distribution for various estimation of Prandtl number for opposing, assisting and steady-state cases. Thermal conductivity decreases by intensifying the Prandtl number, therefore, temperature profiles decrease. The changes in the temperature profiles for different estimations of space and temperature dependent uneven energy gain or loss are plotted in Figs. 3(e) and 3(f). It is mentioned that the positive values of space and temperature dependent parameter are considered as an energy gain whereas negative values of space and temperature dependent parameter are considered as an energy loss, respectively. Due to this reason, the fluid temperature enhances with uplifting values of space and temperature dependent parameter.

Figs. 4(a-c) portray the impact of concentration on various estimations of solutal slip, Schmidt number, and chemical reaction parameter respectively.Fig. 4(a) is plotted to exhibits the impact of solutal slip on concentration distribution for cases of opposing, assisting and steady-state. We see from this assumption that the fixation conveyance of the fluid concentration diminishes as the solutal slip increments. Fig. 4(b) deliberately displays the effect of the *Sc* to the concentration distribution. It is notable that the Schmidt number is the ratio between momentum and mass diffusivities. Therefore the higher value of Schmidt number is equivalent to small mass diffusivity. So concentration profile declines. Fig. 4(c) deliberately displays the $\gamma$ chemical reaction on the concentration profile. It is noteworthy to consider $(\gamma > 0)$ as a destructive chemical reaction and $(\gamma < 0)$ as a generative chemical reaction, respectively. As a result, both types of chemical reaction decline the fluid concentration. A variation on fluid velocity, temperature and concentration for the suction parameter is plotted in Fig. 5. It seems from this figure that the $f', \theta$ and $\phi$ diminish with large values of the suction parameter.

Fig. 6(a-c) shows the influence of $f', \theta$ and $\phi$ on the unsteadiness parameter. Fig. 6(a) demonstrates the impact of the $f'$ that diminishes with the increase of unsteadiness parameter. Unsteadiness parameter changes on $\theta$ are displayed in Fig. 6(b) for opposing and assisting flows. We noticed from this figure that the impact of expanding estimations of the unsteadiness parameter is to diminish the $\theta$.

Fig. 6(c) is intended to reveal insights into the impact of *A* on the $\phi$. It uncovers that the $\phi$ diminishes by uplifted *A*. To validate the accuracy of the this model, we compared the numerical results, corresponding to $-\theta'(0)$ and $\theta'(0)$, with the results previously reported in Refs. [2-7]. These comparision Tables 1 and 2 have a good result. The results of shear stress, rate of heat and mass transfer are given in Table 3. $f''(0)$ rises with large values of *Gr, Gc, F, R, Ec* and $A^*$. $-\theta'(0)$ diminishes with high *M*, *R*, $A^*$, E, Sc and $\gamma$. For large values *Gr, S, A, Sc, R, Gc, Ec,* $\gamma$ and $A^*$ increases the $-\phi'(0)$.

**Table 1.** The variation of $-\theta'(0)$ for some reduced cases when $\gamma = 0$, $M = A = Da = Gr = Gc = Ec = Sc = S_f = S_t = 0 = S_c = 0$.

| | Bidin and Nazar [2] | | Nadeem et al. [3] | | Mukhopadhyay and Reddy [4] | | Present | |
|---|---|---|---|---|---|---|---|---|
| Pr \ R | 0.5 | 1 | 0.5 | 1 | 0.5 | 1 | 0.5 | 1 |
| 1 | 0.6765 | 0.5315 | 0.680 | 0.534 | 0.6765 | 0.5315 | 0.67657 | 0.53155 |
| 2 | 1.0735 | 0.8627 | 1.073 | 0.863 | 1.0734 | 0.8626 | 1.07352 | 0.86277 |
| 3 | 1.3807 | 1.1214 | 1.381 | 1.121 | 1.3807 | 1.1213 | 1.38075 | 1.12143 |

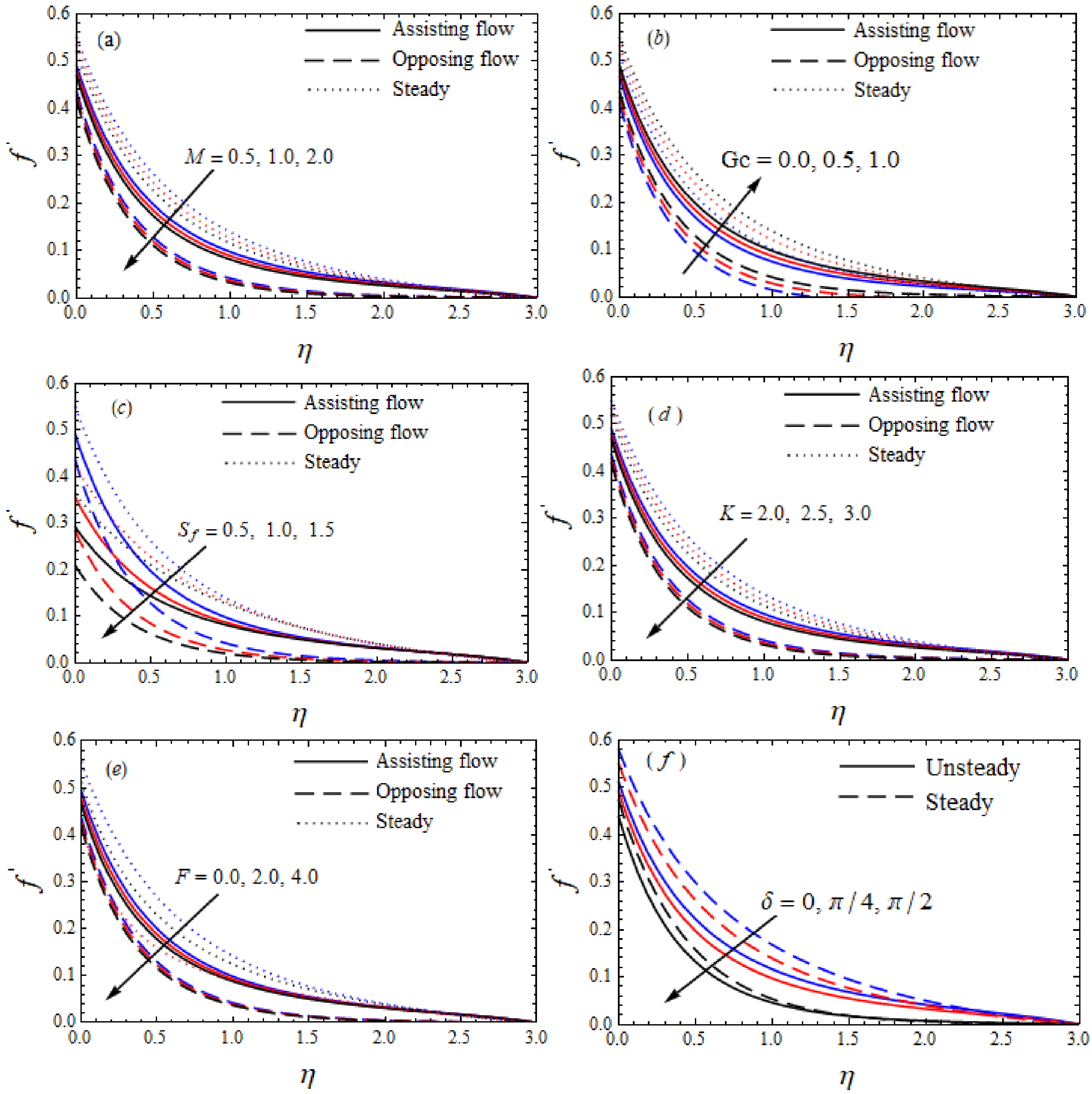


**Fig. 2.** Velocity distribution (a) Variation of $M$, (b) Variation of $Gc$, (c) Variation of $S_f$, (d) Variation of $K$, (e) Variation of $F$ and (f) Variation of $\delta$.

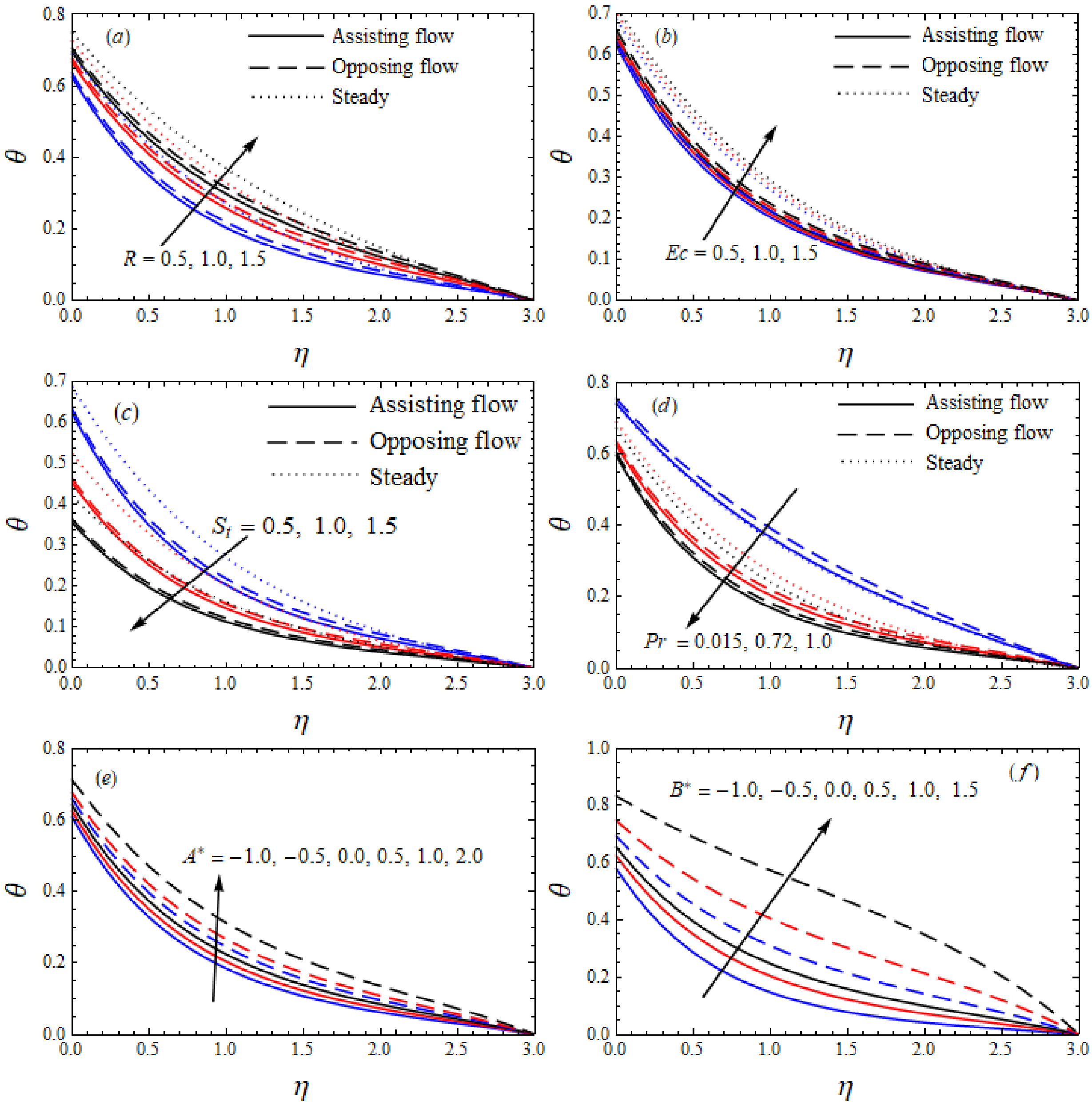


**Fig. 3.** Temperature distribution (a) Variation of $R$, (b) Variation of $Ec$, (c) Variation of $S_t$, (d) Variation of $Pr$, (e) Variation of $A^*$ and (f) Variation of $B^*$.

**Table 2.** The variation of $\theta'(0)$ for some reduced cases when $\gamma = 0$, $M = A = Da = Gr = Gc = R = Ec = Sc = S_f = S_t = 0 = S_c = 0$.

| Pr | Magyari and Keller [5] | Al-Odat et al. [6] | Pal [7] | Present |
|---|---|---|---|---|
| 0.5 | -0.59434 | -0.91903 | -0.59434 | -0.59436 |
| 1 | -0.95478 | -0.57771 | -0.95478 | -0.95478 |
| 3 | - 1.86908 | -1.81039 | -1.86907 | -1.86693 |
| 5 | -2.50014 | -2.28864 | -2.50013 | -2.50014 |
| 8 | -3.24213 | -3.00587 | -3.24212 | -3.24214 |
| 10 | -3.66038 | -3.18620 | -3.66037 | -3.66037 |

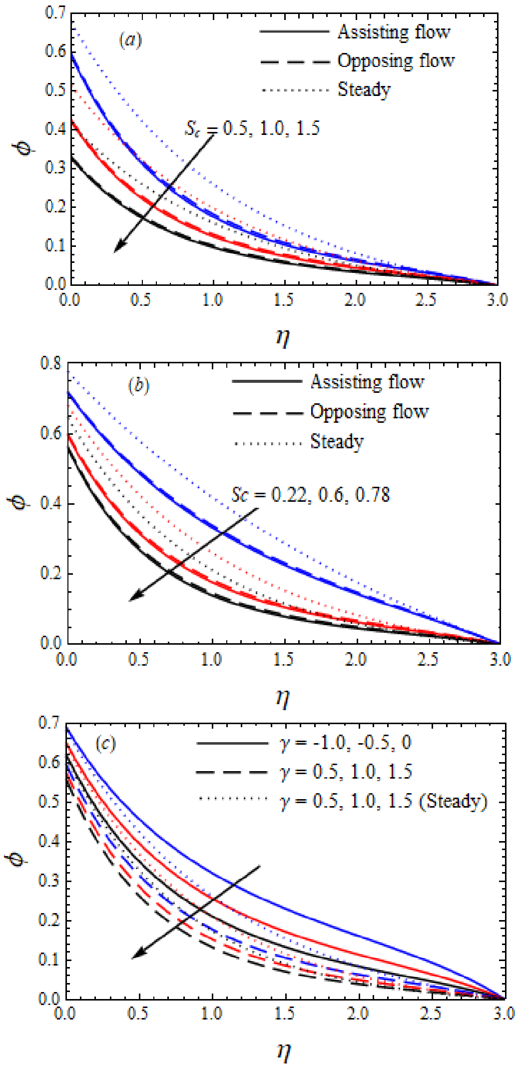


**Fig. 4.** Concentration distribution (a) Variation of $S_c$, (b) Variation of $Sc$ and (c) Variation of $\gamma$ .

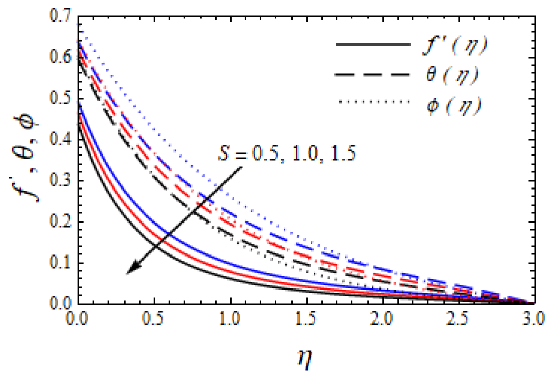


**Fig. 5.** Velocity, temperature and concentration distributions for variation of S.

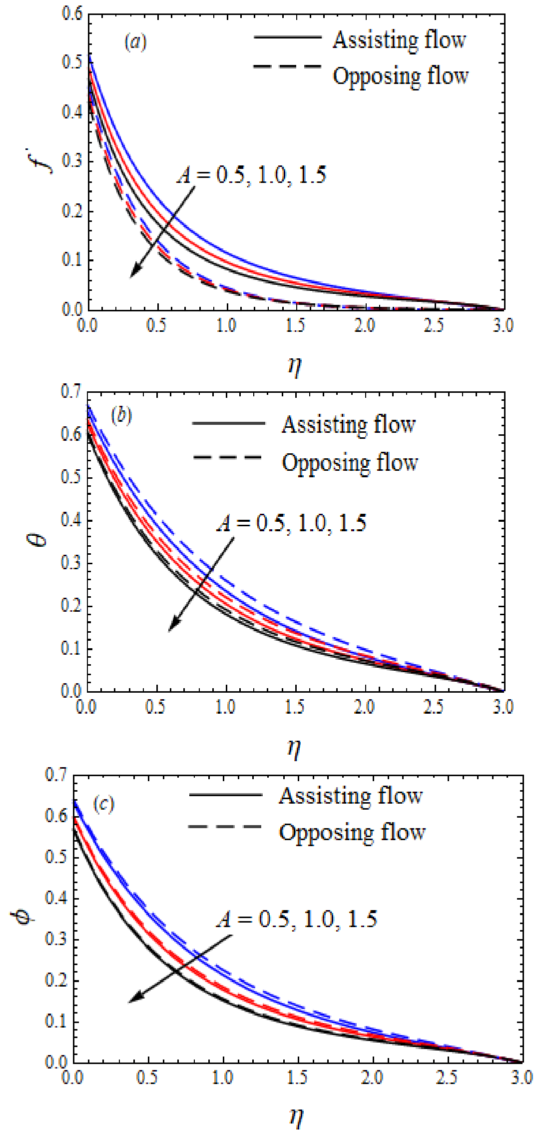


**Fig. 6.** Variation of A on (a) Velocity (b) temperature and (c) concentration distributions.

## 4. Conclusions

The main goal of this investigation is to exhibit the Darcy-Forchheimer flow of chemically reacting viscous fluid over an inclined exponentially preamble stretching sheet. It is found that velocity, thermal and concentration-related boundary layer thickness declined by uplifted values of a time-dependent parameter. The velocity diminishes with large values of the inclination parameter for both unsteady and steady cases. Temperature increments with large values of the non-uniform heat source; though

**Table 3.** Changes of $f''(0)$, $-\theta'(0)$ and $-\phi'(0)$ for uplifted values of *Gr*, *Gc*, $f_0$, *M*, *A*, *K*, *F*, *R*, *Pr*, $A^*$, $B^*$, Ec, Sc, and $\gamma$ when $S_f = S_t = S_c = 0.5$, and $\delta = 45^o$.

| Gr | Gc | $f_0$ | *M* | *A* | *K* | *F* | R | Pr | $A^*$ | $B^*$ | *Ec* | Sc | $\gamma$ | $f''(0)$ | $-\theta'(0)$ | $-\phi'(0)$ |
|---|---|---|---|---|---|---|---|---|---|---|---|---|---|---|---|---|
| 1.0 | 1.0 | 0.5 | 1.0 | 1.0 | 2.0 | 0.5 | 0.5 | 0.72 | 0.5 | 0.5 | 0.5 | 0.6 | 0.5 | -1.001470 | 0.520708 | 0.811907 |
| 2.0 | 1.0 | 0.5 | 1.0 | 1.0 | 2.0 | 0.5 | 0.5 | 0.72 | 0.5 | 0.5 | 0.5 | 0.6 | 0.5 | -0.930696 | 0.522769 | 0.817644 |
| 1.0 | 2.0 | 0.5 | 1.0 | 1.0 | 2.0 | 0.5 | 0.5 | 0.72 | 0.5 | 0.5 | 0.5 | 0.6 | 0.5 | -0.953866 | 0.521791 | 0.815431 |
| 1.0 | 1.0 | 1.0 | 1.0 | 1.0 | 2.0 | 0.5 | 0.5 | 0.72 | 0.5 | 0.5 | 0.5 | 0.6 | 0.5 | -1.055120 | 0.575950 | 0.864559 |
| 1.0 | 1.0 | 0.5 | 2.0 | 1.0 | 2.0 | 0.5 | 0.5 | 0.72 | 0.5 | 0.5 | 0.5 | 0.6 | 0.5 | -1.048610 | 0.519833 | 0.808560 |
| 1.0 | 1.0 | 0.5 | 1.0 | 2.0 | 2.0 | 0.5 | 0.5 | 0.72 | 0.5 | 0.5 | 0.5 | 0.6 | 0.5 | -0.509886 | 0.714610 | 0.907271 |
| 1.0 | 1.0 | 0.5 | 1.0 | 1.0 | 3.0 | 0.5 | 0.5 | 0.72 | 0.5 | 0.5 | 0.5 | 0.6 | 0.5 | -1.048610 | 0.519833 | 0.808560 |
| 1.0 | 1.0 | 0.5 | 1.0 | 1.0 | 2.0 | 1.0 | 0.5 | 0.72 | 0.5 | 0.5 | 0.5 | 0.6 | 0.5 | -1.010010 | 0.520691 | 0.811400 |
| 1.0 | 1.0 | 0.5 | 1.0 | 1.0 | 2.0 | 0.5 | 1.0 | 0.72 | 0.5 | 0.5 | 0.5 | 0.6 | 0.5 | -0.996987 | 0.468829 | 0.812351 |
| 1.0 | 1.0 | 0.5 | 1.0 | 1.0 | 2.0 | 0.5 | 0.5 | 1.0 | 0.5 | 0.5 | 0.5 | 0.6 | 0.5 | -1.010490 | 0.626750 | 0.811012 |
| 1.0 | 1.0 | 0.5 | 1.0 | 1.0 | 2.0 | 0.5 | 0.5 | 0.72 | 1.0 | 0.5 | 0.5 | 0.6 | 0.5 | -0.997548 | 0.473498 | 0.812294 |
| 1.0 | 1.0 | 0.5 | 1.0 | 1.0 | 2.0 | 0.5 | 0.5 | 0.72 | 0.5 | 1.0 | 0.5 | 0.6 | 0.5 | -0.989559 | 0.389880 | 0.813141 |
| 1.0 | 1.0 | 0.5 | 1.0 | 1.0 | 2.0 | 0.5 | 0.5 | 0.72 | 0.5 | 0.5 | 1.0 | 0.6 | 0.5 | -0.999642 | 0.493358 | 0.812068 |
| 1.0 | 1.0 | 0.5 | 1.0 | 1.0 | 2.0 | 0.5 | 0.5 | 0.72 | 0.5 | 0.5 | 0.5 | 1.0 | 0.5 | -1.011860 | 0.520266 | 0.956305 |
| 1.0 | 1.0 | 0.5 | 1.0 | 1.0 | 2.0 | 0.5 | 0.5 | 0.72 | 0.5 | 0.5 | 0.5 | 0.6 | 1.0 | -1.004670 | 0.520565 | 0.852594 |

the turnaround pattern is seen in the case of the sink. The effect of large estimations of Eckert number is to increase the temperature distribution. The outcomes relating to the present investigation demonstrate that due to solutal slip, the concentration diminishes. The skin-friction coefficient is high for the large values of the Grashof number. The local Nusselt number was found to be decreasing as the value of the Eckert number increases.

## References


[1] L. J. Crane, "Flow past a stretching plate", *Zeitschrift für Angew. Math. und Phys. ZAMP*, Vol. 21, No. 4, pp. 645-647, (1970).

[2] B. Bidin and R. Nazar, "Numerical solution of the boundary layer flow over an exponentially stretching sheet with thermal radiation", *Eur. J. Sci. Res.*, Vol. 33, No. 4, pp. 710-717, (2009).

[3] S. Nadeem, S. Zaheer and T. Fang, "Effects of thermal radiation on the boundary layer flow of a Jeffrey fluid over an exponentially stretching surface", *Numer. Algorithms*, Vol. 57, No. 2, pp. 187-205, (2011).

[4] S. Mukhopadhyay and R. S. R. Gorla, "Effects of partial slip on boundary layer flow past a permeable exponential stretching sheet in presence of thermal radiation", *Heat Mass Transf.*, Vol. 48, No. 10, pp. 1773-1781, (2012).

[5] E. Magyari and B. Keller, "Heat and mass transfer in the boundary layers on an exponentially stretching continuous surface", *J. Phys. D. Appl. Phys.*, Vol. 32, No. 5, pp. 577-585, (1999).

[6] M. Q. Al-Odat, R. A. Damseh and T. A. Al-Azab, "Thermal boundary layer on an exponentially stretching continous surface in the presence of magnetic field effect", *Int. J. Appl. Mech. Eng.*, Vol. 11, No. 2, pp. 289-299, (2006).

[7] D. Pal, "Mixed convection heat transfer in the boundary layers on an exponentially stretching surface with magnetic field", *Appl. Math. Comput.*, Vol. 217, No. 6, pp. 2356-2369, (2010).

[8] M. Abd El-Aziz, "Viscous dissipation effect on mixed convection flow of a micropolar fluid over an exponentially stretching sheet", *Can. J. Phys.*, Vol. 87,

No. 4, pp. 359-368, (2009).

[9] M. Sajid and T. Hayat, "Influence of thermal radiation on the boundary layer flow due to an exponentially stretching sheet", *Int. Commun. Heat Mass Transf.*, Vol. 35, No. 3, pp. 347-356, (2008).

[10] R. Cortell, "Combined effect of viscous dissipation and thermal radiation on fluid flows over a non-linearly stretched permeable wall", *Meccanica*, Vol. 47, No. 3, pp. 769-781, (2012).

[11] P. H. Veena, S. Abel, K. Rajagopal and V. K. Pravin, "Heat transfer in a visco-elastic fluid past a stretching sheet with viscous dissipation and internal heat generation", *Zeitschrift fur Angew. Math. und Phys.*, Vol. 57, No. 3, pp. 447-463, (2006).

[12] S. R. R. Reddy and P. Bala Anki Reddy, "Bio-mathematical analysis for the stagnation point flow over a non-linear stretching surface with the second order velocity slip and titanium alloy nanoparticle", *Front. Heat Mass Transf.*, Vol. 10, No. 13, pp. 1-11, (2018).

[13] S. Gupta, D. Kumar and J. Singh, "MHD mixed convective stagnation point flow and heat transfer of an incompressible nanofluid over an inclined stretching sheet with chemical reaction and radiation", *Int. J. Heat Mass Transf.*, Vol. 118, pp. 378-387, (2018).

[14] A. Saadatmandi and Z. Sanatkar, "Collocation method based on rational Legendre functions for solving the magneto-hydrodynamic flow over a nonlinear stretching sheet", *Appl. Math. Comput.*, Vol. 323, pp. 193-203, (2018).

[15] P. Kumar, K. Tanmoy and C. Kalidas, "Framing the Cattaneo – Christov heat flux Phenomena on CNT- based Maxwell Nanofluid along stretching sheet with multiple slips", *Arab. J. Sci. Eng.*, Vol. 43, No. 3, pp. 1177-1188, (2018).

[16] P. B. A. Reddy and N. B. Reddy, "Thermal radiation effects on hydro-magnetic flow due to an exponentially stretching sheet", *Int. J. Appl. Math. Comput.*, Vol. 3, No. 4, pp. 300-306, (2011).

[17] M. M. Bhatti, M. A. Abbas and M. M. Rashidi, "A robust numerical method for solving stagnation point flow over a permeable shrinking sheet under the influence of MHD", *Appl. Math. Comput.*, Vol. 316, pp. 381-389, (2018).

[19] S. R. R. Reddy, P. Bala Anki Reddy and S. Suneetha, "Magnetohydrodynamic flow of blood in a permeable inclined stretching surface with viscous dissipation, non-uniform heat source/sink and chemical reaction", *Front. Heat Mass Transf.*, Vol. 10, No. 22, pp. 1-10, (2018).

[20] K. Vajravelu, K. V. Prasad and C. O. Ng, "Unsteady convective boundary layer flow of a viscous fluid at a vertical surface with variable fluid properties", *Nonlinear Anal. Real World Appl.*, Vol. 14, No. 1, pp. 455-464, (2013).

[21] P. B. A. Reddy and N. B. Reddy, "Finite difference analysis of radiation effects on unsteady MHD flow of a chemically reacting fluid with time-dependent suction", *Int. J. Appl. Math Mech.*, Vol. 7, No. 9, pp. 96-105, (2011).

[22] A. J. Chamkha, A. M. Aly and M. A. Mansour, "Similarity solution for unsteady heat and mass transfer from a stretching surface embedded in a porous medium with suction / injection and chemical reaction effects", *Chem. Eng. Commun.*, Vol. 197, No. 6, pp. 846-858, (2010).

[23] D. Pal and N. Roy, "Lie group transformation on MHD double-diffusion convection of a Casson nanofluid over a vertical stretching / shrinking surface with thermal radiation", *Int. J. Appl. Comput. Math.*, Vol. 13, No. 4, pp. 1-23, (2018).

[24] N. Bachok, A. Ishak and I. Pop, "Unsteady boundary-layer flow and heat transfer of a nanofluid over a permeable stretching/shrinking sheet", *Int. J. Heat Mass Transf.*, Vol. 55, No. 7-8, pp. 2102-2109, (2012).

[25] D. Pal, "Combined effects of non-uniform heat source/sink and thermal radiation on heat transfer over an

unsteady stretching permeable surface", *Commun. Nonlinear Sci. Numer. Simul.*, Vol. 16, No. 4, pp. 1890-1904, (2011).

[26] J. C. Misra and A. Sinha, "Effect of thermal radiation on MHD flow of blood and heat transfer in a permeable capillary in stretching motion", *Heat Mass Transf.*, Vol. 49, No. 5, pp. 617-628, (2013).

[27] S. Srinivas, P. B. A. Reddy and B. S. R. V. Prasad, "Non-Darcian unsteady flow of a micropolar fluid over a porous stretching sheet with thermal radiation and chemical reaction", *Heat Transf. Res.*, Vol. 44, No. 2, pp. 172-187, (2015).

[28] Yan Zhang, Min Zhang and Shujuan Qi, "Heat and mass transfer in a thin liquid film over an unsteady stretching surface in the presence of thermo solutal capillarity and variable magnetic field", *Math. Probl. Eng.,* Vol. 2016, pp. 8521580, (2016).

[29] M. Hatami, Kh. Hosseinzadeh, G. Domairry and M. T. Behnamfar, "Numerical study of MHD two-phase Couette flow analysis for fluid-particle suspension between moving parallel plates", *J Taiwan Inst Chem Eng,* Vol. 45, No. 5, 2238-2245, (2014).

[30] S. S. Ghadikolaei, Kh. Hosseinzadeh and D. D. Ganji, "Analysis of unsteady MHD Eyring-Powell squeezing flow in stretching channel with considering thermal radiation and Joule heating effect using AGM", *Case Stud. Therm. Eng.,* Vol. 10 pp. 579-594, (2017).

[31] K. Das, "Slip flow and convective heat transfer of nanofluids over a permeable stretching surface", *Comput. Fluids* Vol. 64, pp. 34-42, (2012).

[32] M. Swati, "Slip effects on MHD boundary layer flow over an exponentially stretching sheet with suction/blowing and thermal radiation", *Ain Shams Eng. J.* Vol. 4, pp. 485-491, (2013).

**How to cite this paper:**

S. R. R. Reddy and P. B. A. Reddy, *"*Impact of thermal radiation and viscous dissipation on hydromagnetic unsteady flow over an exponentially inclined preamble stretching sheet*", Journal of Computational and Applied Research in Mechanical Engineering,* Vol. 10, No. 1, pp. 171-181, (2020).

**DOI:** 10.22061/jcarme.2019.3709.1433

**URL:** http://jcarme.sru.ac.ir/?_action=showPDF&article=1144